Remote Sensing of Environment 145 (2014) 38–46

Contents lists available at ScienceDirect

Remote Sensing of Environment

journal homepage: www.elsevier.com/locate/rse

Satellite bio-optical and altimeter comparisons of phytoplankton blooms induced by natural and artificial iron addition in the Gulf of Alaska

Peng Xiu [a,b,*], Andrew C. Thomas [a], Fei Chai [a]

[a] School of Marine Sciences, University of Maine, Orono, ME 04469, United States
[b] State Key Laboratory of Tropical Oceanography, South China Sea Institute of Oceanography, Chinese Academy of Sciences, Guangzhou, China

ARTICLE INFO

Article history:
Received 20 February 2013
Received in revised form 20 December 2013
Accepted 2 February 2014
Available online xxxx

Keywords:
Iron fertilization
HNLC
Eddy
Volcano
Iron limitation
Remote sensing data
Chlorophyll
Phytoplankton

ABSTRACT

An iron fertilization experiment conducted during the summer of 2012 dumped over 100 tons of an iron-containing substance into surface waters of a Haida eddy in the eastern North Pacific to stimulate a large phytoplankton bloom. Announced as a privately funded ocean fertilization effort to increase salmon returns, it attracted considerable press coverage, caused much public controversy and has been widely denounced by the science community. Here, we use available satellite bio-optical measurements from the MODIS/Aqua instrument and AVISO altimeter dynamic height data to examine the timing, magnitude and extent of this artificial iron fertilization experiment, comparing it with natural fertilization events such as volcanic ash deposition and mesoscale eddy transport in the Gulf of Alaska. With respect to other Haida eddies over the past 10 years, this event produced the highest chlorophyll concentrations observed late (>400 days) in eddy life history, produced the strongest bloom ever observed in an eddy in late-summer and induced this late-summer bloom earlier in the season than any other eddy. With respect to the local area of the fertilization, this experiment induced the most intensive phytoplankton bloom of the past 10 years, ~2× stronger than that caused by Kasatochi volcano in 2008, ~5× that typically observed in the region, including any induced by passing eddies of previous years. Due to its limited spatial and temporal scales, however, estimated total annual carbon drawdown over the Gulf of Alaska by this experiment is one order of magnitude smaller than the Kasatochi volcano and mesoscale Haida eddies. The target eddy followed a path typical of previous Haida eddies, but with relatively weak dynamic height and rotational circulation. Satellite-based calculations also suggest that only a small fraction of the dumped iron might have been taken up by phytoplankton. The extent to which this localized experiment may impact higher trophic levels such as salmon remains uncertain.

1. Introduction

Iron limitation on phytoplankton growth, ocean productivity and its role in biogeochemical cycles and global climate was first proposed by John Martin (1990). Since then, this "Iron Hypothesis" has been systematically tested by mesoscale iron addition experiments conducted in a number of high-nutrient, low-chlorophyll (HNLC) regions of the ocean (e.g., Boyd et al., 2007; Coale et al., 2004). These studies provide insights into the nutrient dynamics upon iron addition, timescales of phytoplankton response and bloom development, ecosystem response and carbon export processes across a wide range of environmental conditions. It has been demonstrated that, especially in these HNLC regions, relaxation of iron limitation is important in modulating phytoplankton growth and biomass and, at least at the lowest trophic levels, food web structure (e.g., de Baar et al., 2005).

The Gulf of Alaska (GoA) in the eastern subarctic Pacific is highly productive in the coastal region. The general circulation in the GoA is dominated by a cyclonic gyre in the central basin, bounded by the North Pacific Current in the south, the Alaska Current in the northeast, and the Alaska Stream in the northwest. In contrast to the productive coastal region, biological activity in the central GoA is much less. The interior of the gyre is characterized as an HNLC area where phytoplankton production in the surface waters is persistently limited by iron concentration, despite strong macro-nutrient input from deep water due to local upwelling and mixing. The Subarctic Ecosystem Response to Iron Enrichment Study (SERIES) conducted at Ocean Station Papa (50°N, 145°W), in the center of the gyre, in 2002 confirmed that iron supply plays a key role in controlling phytoplankton concentrations in this region (Boyd et al., 2004).

In the GoA HNLC area, surface iron concentrations are typically below 0.05 nM, about two orders of magnitude lower than those in the coastal region (Johnson, Miller, Sutherland, & Wong, 2005; Nishioka, Takeda, Wong, & Johnson, 2001). Sources of iron in coastal regions are thought to be largely contributed by terrestrial runoff, rivers, and shelf sediment re-suspension (Stabeno et al., 2004). Unlike the shelf regions, however, the HNLC waters in the central gyre receive little iron from coastal waters due to the weak cross-gyre current flow. Previous studies show that there are at least three major sources of iron for

* Corresponding author at: 5706 Aubert Hall, Orono, Maine 04469, USA. Tel.: +1 207 5814349.
E-mail address: peng.xiu@maine.edu (P. Xiu).

http://dx.doi.org/10.1016/j.rse.2014.02.004
0034-4257/

the central GoA HNLC area. One is via atmospheric dust deposition originating from either the Asian continent or Alaskan volcanic activity (Bishop, Davis, & Sherman, 2002; Boyd et al., 1998; Duce & Tindale, 1991; Hamme et al., 2010; Jickells et al., 2005). Another is via the lateral transport of particulate iron from the continental margin (Lam et al., 2006). The other supply mechanism is transport by mesoscale anticyclonic eddies. These eddies move coastal iron-rich waters across the continental shelf, into the open ocean, providing a significant contribution to the iron budget of the central GoA (Combes, Di Lorenzo, & Curchitser, 2009; Crawford, Brickley, & Thomas, 2007; Johnson et al., 2005; Xiu, Palacz, Chai, Roy, & Wells, 2011; Xiu, Chai, Xue, Shi, & Chao, 2012). Among the three types of eddies recognized in the GoA, Haida eddies generally form at the shelf break off Haida Gwaii, Canada, between winter and spring and move offshore (Crawford, 2002; Henson & Thomas, 2008).

Announced as an effort to increase salmon returns, the Haida Salmon Restoration Corporation (HSRC) conducted an iron fertilization experiment during the summer of 2012 by dumping over 100 tons of iron (finely-ground dirt-like substance) into a Haida eddy. The first report about the project appeared in the newspaper, The Guardian (Lukacs, 2012). After that, different media articles followed up, causing considerable controversy and wide-spread denouncement by scientists due to the unknown ecological impacts (e.g., Service, 2012; Tollefson, 2012). An assessment of this experiment in terms of local fish returns will not be possible for two or three years when the adult salmon return to the Haida region. Even then, a quantitative demonstration of direct causality would be difficult. Determining the local effects of iron fertilization against the background natural variations is also difficult. At present, we are not aware of any publically available in-situ data from the experiment. With satellite remote sensing measurements, however, we can estimate some of the immediate surface biological responses to the artificial iron addition and contrast these with other eddies, climatological patterns in the region and other iron inputs. One of the scientific controversies of this experiment is the interaction between biological responses to natural iron carried within the Haida eddy and the artificial iron dumped into the upper ocean (e.g., Strutton, 2012). Here we use available multi-platform remote sensing tools to provide an initial overview of the local physical environment and its biological response to the fertilization, and compare these to earlier, natural fertilization events and natural variability.

2. Methods and data

Daily satellite altimeter-measured sea level anomaly (SLA) fields, produced and distributed by AVISO (http://www.aviso.oceanobs.com/) for the period of 2002–2012 were acquired and subset to the study area. Following methodologies applied in previous studies (Henson & Thomas, 2008; Xiu et al., 2012), mesoscale eddies were identified and tracked in time using the Okubo–Weiss (O-W) method. During each time step, the velocity field is derived from SLA maps assuming geostrophic balance:

$$u = -\frac{g}{f}\frac{\partial h}{\partial y}, \quad v = \frac{g}{f}\frac{\partial h}{\partial x} \tag{1}$$

where h is the SLA, g is the gravitational acceleration, and f is the Coriolis parameter. The O-W parameter of a two-dimensional disturbance field is defined by

$$W = s_n^2 + s_s^2 - \omega^2 \tag{2}$$

where s_n is the normal component of strain, s_s is the shear component, and ω is the relative vorticity of the flow, defined by, respectively

$$s_n = \frac{\partial u}{\partial x} - \frac{\partial v}{\partial y}, \qquad s_s = \frac{\partial v}{\partial x} + \frac{\partial u}{\partial y}, \qquad \omega = \frac{\partial v}{\partial x} - \frac{\partial u}{\partial y}. \tag{3}$$

The O-W parameter, W, separates the flow field into either strain-dominated ($W > 0$) or vorticity-dominated ($W < 0$) regions. We define the eddy core as a coherent region with a high vorticity threshold ($W < -0.2\sigma_w$), where σ_w is the standard deviation of W, obtained from each time step of the study area. Eddy trajectories are determined from map to map using a connectivity algorithm that identifies the groups of pixels that are adjacent in longitude, latitude, and time. Two eddies in two consecutive maps are considered as the same one if the edges of these two eddies are connected. In this study, we only consider the long-lived mesoscale eddies formed in the Haida region (Fig. 1) with diameters larger than 60 km and lifespans longer than 200 days.

Eight-day and monthly composite satellite ocean color products from the NASA MODIS/Aqua instrument, including chlorophyll concentration, particulate organic carbon (POC), remote-sensing reflectance at 555 nm (Rrs555), colored dissolved organic matter (CDOM) index, and normalized fluorescence line height (NFLH), all with a horizontal resolution of 4 km, were obtained from the NASA ocean color data archive (http://oceancolor.gsfc.nasa.gov/; Feldman & McClain, 2009) and used to assess biological consequences of the iron addition in the upper ocean. In order to evaluate phytoplankton chlorophyll-to-carbon ratio changes during the iron addition, phytoplankton chlorophyll and carbon concentrations measured by the MODIS sensor and calculated with the GSM algorithm were obtained from the ocean productivity website (http://www.science.oregonstate.edu/ocean.productivity; Westberry, Behrenfeld, Siegel, & Boss, 2008).

3. Results and discussion

Press coverage and examination of MODIS ocean color data allowed us to identify the approximate location of the iron experiment. Using the altimeter data, we tracked the target eddy back in time and space to April 2011, when it first detached from the southern tip of Haida Gwaii. After formation, this eddy (eddy A) moved in a generally northwest direction. Five months later (Fig. 1a), another eddy (eddy B) was generated at a similar location and propagated northwest following a similar path. Eddy B interacted with, and eventually merged with eddy A in January 2012, providing a potential refill of iron-rich shelf water to eddy A. In August 2012, a new eddy formed at approximately 226°E, 52.5°N (Fig. 1b). By August 2012, when artificial iron was added to eddy A, it was about 16-months old with a sea level anomaly (SLA) of less than 6 cm at its center. Altimeter expressions of eddy A eventually disappeared in January 2013. Surface layer chlorophyll concentrations detected by MODIS/Aqua indicate anomalously high levels at the core of eddy A when compared with the same region in 2011 (Fig. 1a and b).

The O-W algorithm tracked 24 long-lived mesoscale eddies in total in the Haida region during period 2002–2012 (Fig. 2). This averages 2.2 eddies per year, consistent with previous studies (Henson & Thomas, 2008; Xiu et al., 2011). Most of the Haida eddies form near the shelf and move westward into the central GoA. The trajectories of eddy A and B are similar to those of other Haida eddies. Table 1 summarizes the mean eddy properties. The average eddy duration is 382 days. Their magnitude, defined as the maximum surface SLA value over the eddy core at each time step and then averaged over the life history, averages ~14.0 cm. The mean eddy propagation speed is estimated to be 2.0 km d^{-1}, and the mean eddy core diameter is ~96.3 km (calculated assuming a radially symmetrical eddy core). This diameter represents only the eddy core region and excludes the outer periphery, making it smaller than the ~150–200 km diameters reported in previous papers (Crawford, 2005). Overall, the eddy duration, magnitudes, and propagation speeds are all in good agreement with previous studies (Henson & Thomas, 2008; Ladd, 2007). In comparison to other Haida eddies, eddy A has a considerably longer lifespan and a relatively weaker surface elevation that would result in a weaker rotation. One consequence of the weak rotation would be poor retention of elevated chlorophyll concentrations in

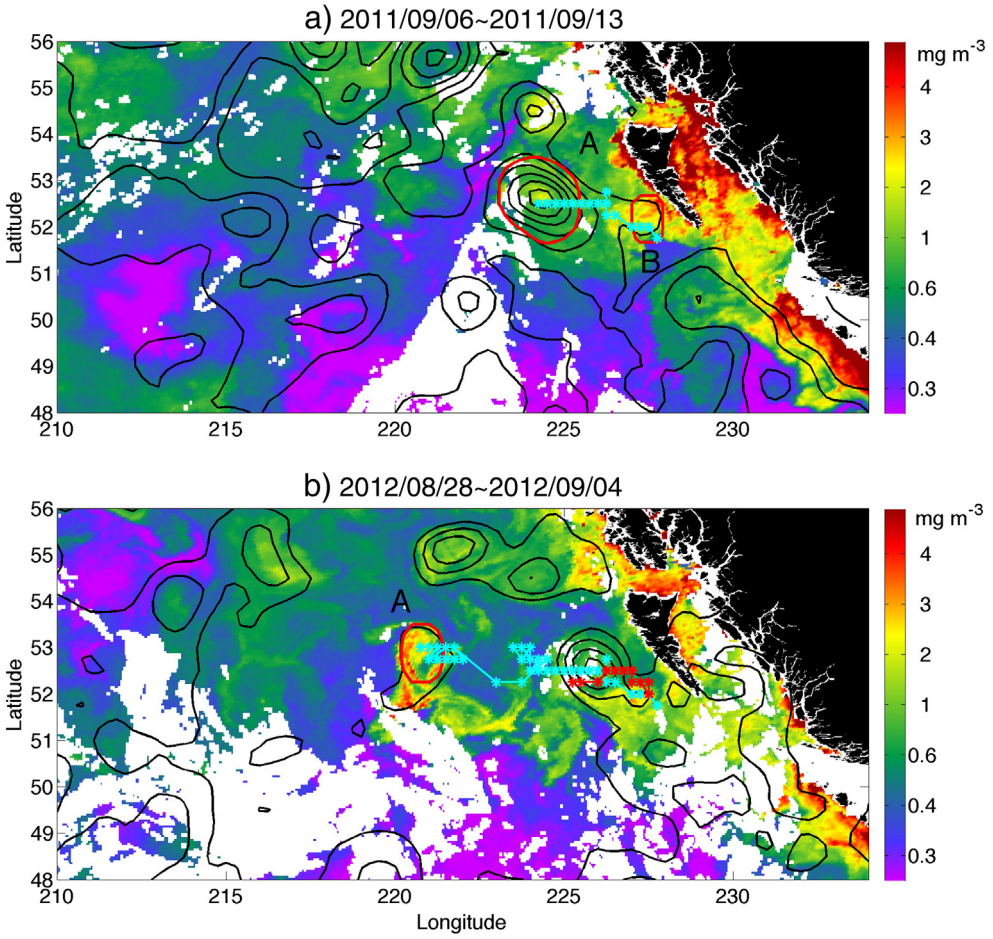

Fig. 1. The MODIS/Aqua derived surface chlorophyll concentrations over the Gulf of Alaska target area for two 8-day composite periods, (a) September 06–13 2011 and (b) August 28–September 04 2012. Black contours show merged SLA data (only positive values). For the same periods, red contours outline the eddy core. Cyan dotted lines denote the track of eddy A and red dotted lines denote the track of eddy B. (For interpretation of the references to color in this figure legend, the reader is referred to the web version of this article.)

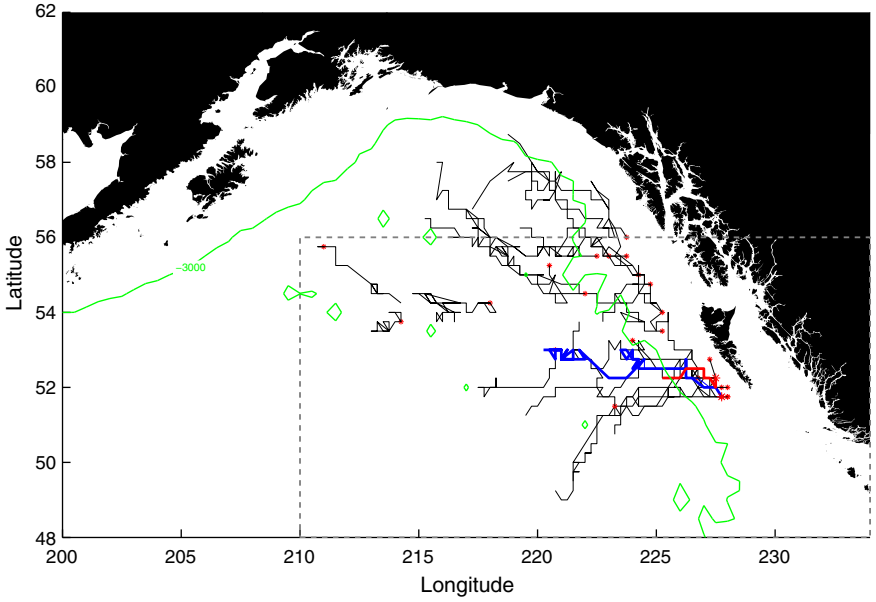

Fig. 2. Tracks (black lines) of those long-lived mesoscale eddies (lifetime > 200 d, diameter > 60 km) formed in the Haida region (48°N–56°N, 210°E–234°E; dashed lines) during 2002–2012. Red asterisks are used to show the starting positions of the eddies. Blue bold line denotes the track of eddy A and red bold line denotes the track of eddy B. Green contour marks the 3000 m isobaths. (For interpretation of the references to color in this figure legend, the reader is referred to the web version of this article.)

Table 1
Altimeter-derived comparisons of eddy A with mean (2002–2012) eddy statistics in the Haida region (for those with lifetimes >200 d and diameter >60 km). The absolute range of parameter values for 2002–2012 is shown in parentheses.

Eddy parameter	Eddy A	Mean eddies
Core diameter [km]	96.2	96.3 (67.2–228.0)
Duration [days]	645	382 (224–707)
Magnitude [cm]	8.6	14.0 (2.1–34.9)
Speed [km d^{-1}]	2.5	2.0 (0.1–10.0)

its interior with increased advection or mixing with surrounding waters (Chelton, Gaube, Schlax, Early, & Samelson, 2011).

Following the eddy's life history, we calculated the mean eddy surface values of multiple bio-optical variables using MODIS/Aqua data, to provide a Lagrangian perspective of their temporal evolution (Fig. 3). Two significant chlorophyll enhancements, one around September 2011 and another in August 2012 are evident (Fig. 3b). In September 2011, eddy A was about 250 km away from its source water and showed a similar chlorophyll increase as eddy B that was at the coast, suggesting consistent water mass properties between eddy A and coastal waters and a similar biological response. In August 2012 after the artificial fertilization, chlorophyll concentration peaked at 3.3 mg m^{-3}, about 10 times higher than previous months (~0.3 mg m^{-3}) and double the concentration of the 2011 chlorophyll peak (~1.6 mg m^{-3}) that was supported by natural iron input.

Satellite-derived POC, a metric that includes phytoplankton carbon plus other non-algal particles also indicated significant peaks in 2011 and 2012 (Fig. 3c). During the 2011 bloom, the POC values increased from about 120 mg C m^{-3} in August to 250 mg C m^{-3} in September; a comparable enhancement ratio (~2) to that for chlorophyll. In comparison, in the 2012 bloom, POC values increased from about 75 mg C m^{-3} to 240 mg C m^{-3}, an enhancement ratio of ~3 significantly lower than the chlorophyll enhancement ratio (~10). This probably suggests a differing POC composition in the upper ocean with relatively

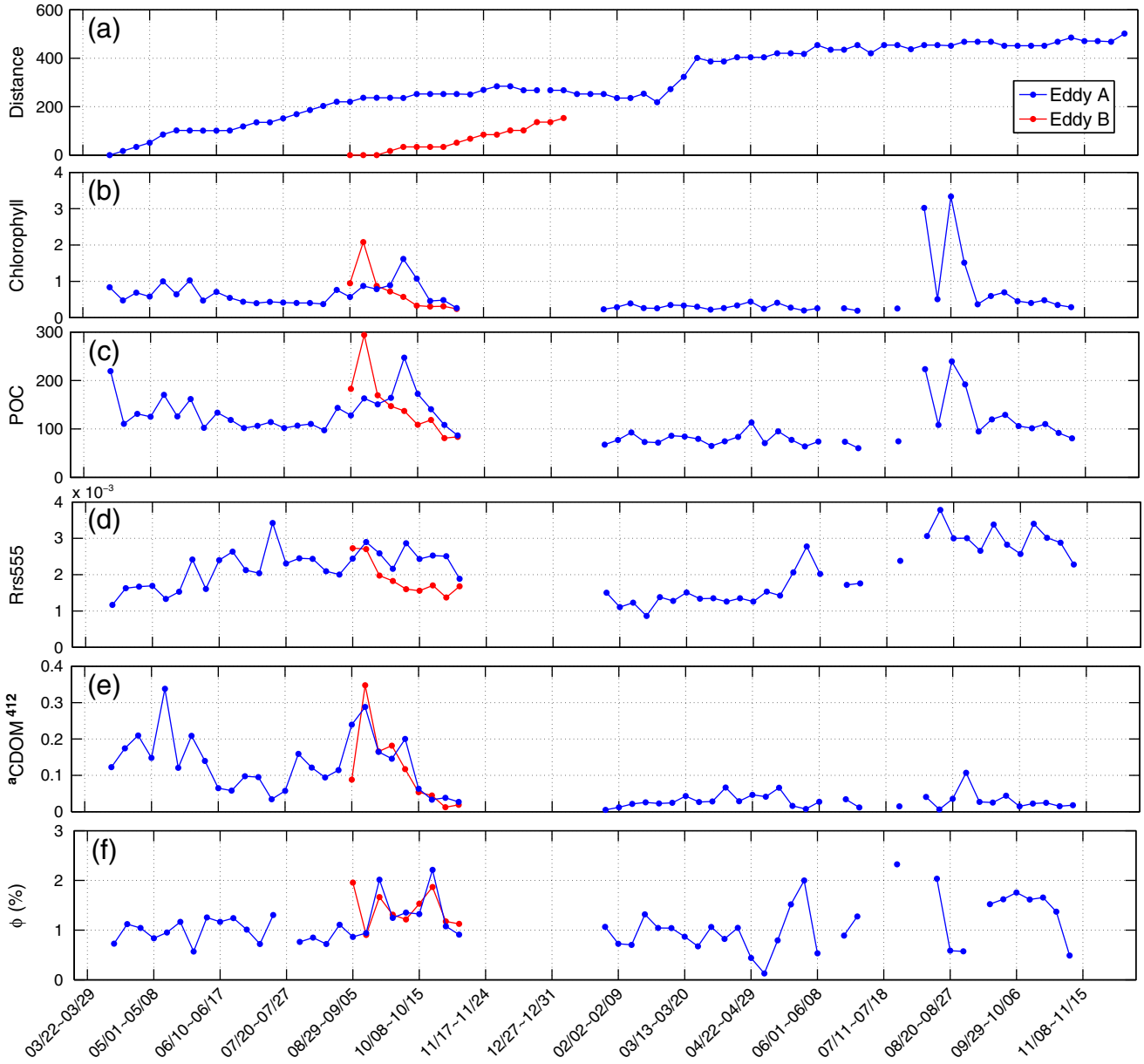

Fig. 3. Lagrangian views of the temporal evolution of satellite-derived characteristics of the target eddy during 2011–2012. Distance (a, km) is calculated between eddy center and its starting location near Haida Gwaii from altimeter data. Time series of MODIS/Aqua derived surface chlorophyll (b, mg m^{-3}), POC (c, mg C m^{-3}), surface turbidity as Rrs555 (d, Sr^{-1}), $a_{CDOM}412$ (e, m^{-1}), and quantum yield of fluorescence ϕ (f, relative) averaged within the eddy core from 8-day composites for eddy A (blue line), and eddy B (red line). (For interpretation of the references to color in this figure legend, the reader is referred to the web version of this article.)

more chlorophyll and fewer non-algal particles in the 2012 bloom than in the 2011 bloom, or an altered phytoplankton carbon-to-chlorophyll ratio due to their physiological adjustments with different growth rates and photoacclimation in the phytoplankton community as discussed in Westberry, Behrenfeld, Milligan, and Doney (2013).

Remote sensing reflectance at 555 nm (Rrs555) was used as an indicator of surface turbidity (e.g., Thomas & Weatherbee, 2006). These data show that surface water turbidity in 2011, when the eddy was close to the shelf, was higher than that early in 2012 (Fig. 3d). The phytoplankton blooms of 2011 and 2012 also induced peaks in turbidity. One interesting feature is that the turbidity peak associated with the 2011 bloom (the natural one) lasted about 40 days before returning to background levels, consistent with the corresponding chlorophyll and POC patterns. In the August 2012 bloom (the artificial one), both the chlorophyll and POC peaks lasted about one month. Turbidity, however, increased and remained high for over two months. In the absence of other measurements, we suggest this high turbidity water results from the dirt-like iron-containing substance or any other material dumped with it into the ocean during the experiment. Considering the typical upper ocean condition with a mixed layer depth about 40 m in this season (Whitney & Freeland, 1999), particles with a maximum sinking velocity of 0.7 m d^{-1} are likely to stay in the upper ocean for two months. This sinking rate is about the magnitude of particles with a size around 10 μm and would be applicable if there was a reasonable component of clay particles in the dumped material. However, how this prolonged and enlarged turbidity within the eddy impacts the regional marine ecosystems remains unknown.

CDOM concentrations are indicative of dissolved organic compounds, usually derived from the degradation of biological material. In the coastal ocean, these are often elevated due to terrestrial inputs, and in the open ocean they result from degradation of planktonic matter. CDOM absorption coefficient at 412 nm ($a_{CDOM}412$) (Fig. 3e) calculated from a satellite-derived CDOM index and chlorophyll concentrations as in Morel and Gentili (2009) shows higher values (>0.05 m^{-1}) in near-shelf waters than in the open ocean (<0.05 m^{-1}). There was a slight increase of CDOM absorption (from 0.15 to 0.2 m^{-1}) during the 2011 bloom while the eddy was about 250 km away its source water. In the 2012 bloom, CDOM absorption indicated a peak (~0.1 m^{-1}) that doubled the level in previous periods (~0.04 m^{-1}). This CDOM peak is later than both the chlorophyll and POC peaks, consistent with a biological origin resulting from the iron-stimulated phytoplankton enhancement.

Normalized fluorescence line height (NFLH) is a measure of chlorophyll fluorescence, an indicator of the efficiency of photosynthesis. It is usually modeled as a product of phytoplankton absorption coefficient, the flux of photosynthetically active radiation (PAR), and the quantum yield of fluorescence. Following previous studies (Behrenfeld et al., 2009), we calculated the quantum yield of fluorescence (ϕ) to qualitatively diagnose surface phytoplankton iron stress (Fig. 3f). As suggested in the global ocean, high fluorescence emissions (ϕ) are found to be associated with strong iron stress due to physiological consequences (Behrenfeld et al., 2009). In 2011, there was a decrease in quantum yield during the phytoplankton bloom and an increase one or two weeks after the bloom with a value of ~2% compared to 1% in previous weeks, suggesting a relief of iron stress during the bloom due to the injection of dissolved iron and an increase of iron stress after the bloom as a result of phytoplankton consuming surface iron. Similarly, there was also a relief of iron stress during the 2012 chlorophyll peak period. After that, an increase of iron stress was evident with high values (>1.5%) maintained for another few weeks probably indicating depletion of dissolved iron in the surface layer.

Over their life history, surface chlorophyll concentrations in the cores of eddy A and B were compared with all other eddies in the Haida region (Fig. 4a). Elevated concentrations are most common early in eddy life. Only one other eddy had chlorophyll concentrations that exceeded 2 mg m^{-3} after the first year of life, and none as late in life as eddy A. To separate variability in chlorophyll concentrations

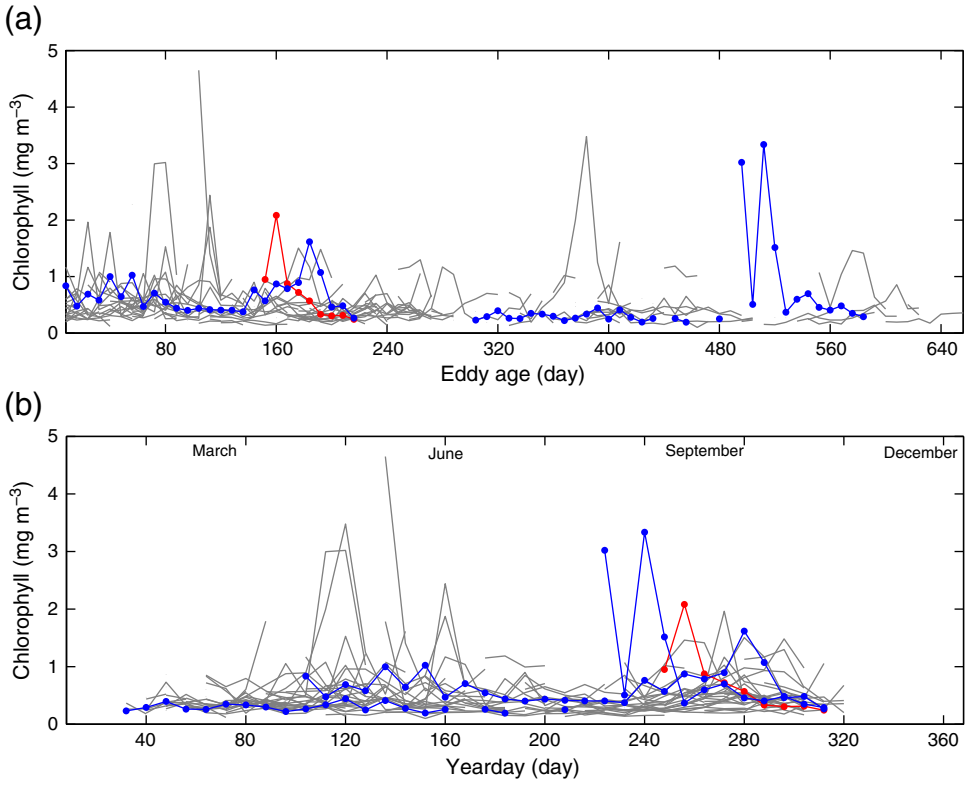

Fig. 4. Mean chlorophyll concentrations in eddy cores for all long-lived Haida eddies (Fig. 2) as a function of eddy age over their entire life history (a) and as a function of yearday (b) to show seasonal changes. Blue and red lines denote concentrations in eddy A and B, respectively. (For interpretation of the references to color in this figure legend, the reader is referred to the web version of this article.)

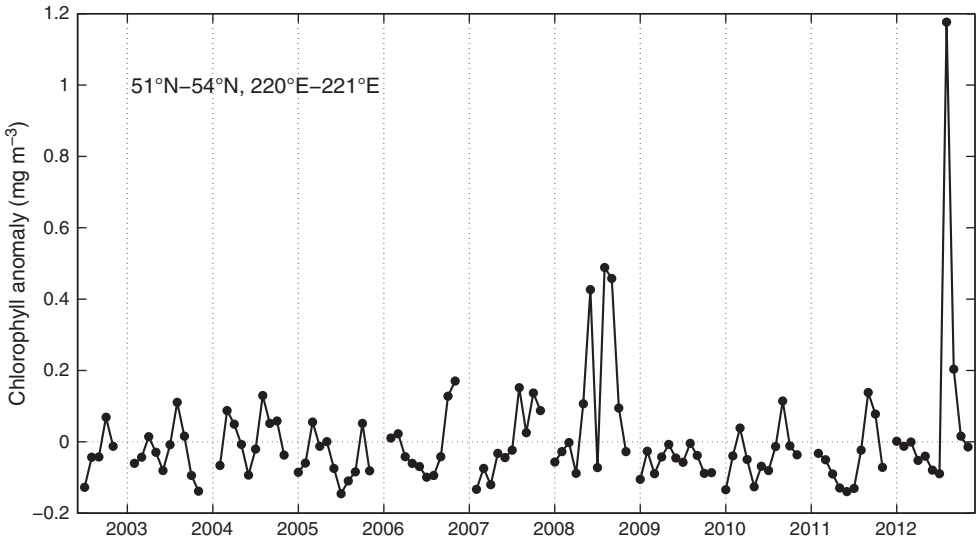

Fig. 5. Monthly surface chlorophyll anomalies (calculated by subtracting climatological monthly mean) averaged over the fertilization experiment region (51°N–54°N, 220°E–221°E) for the period July 2002 to November 2012.

over eddy life history from chlorophyll seasonality, the same data is plotted as a function of yearday (Fig. 4b). Spring and late summer increases are evident in many eddies, but eddy A clearly had the strongest concentrations among those with late summer increases. Furthermore, the late summer increase in eddy A is the earliest in the year of any over the past 10 years. These data illustrate the degree to which chlorophyll concentrations inside eddy A differ from those of natural eddies and further suggests that the 2012 eddy A bloom is an artificial event.

To provide a historical perspective on the magnitude of the artificially-induced bloom of 2012, we calculated monthly surface chlorophyll concentration anomalies (by subtracting the climatological 2002–2012 monthly mean) averaged within a region (51°N–54°N, 220°E–221°E) that encompasses the area of the 2012 bloom at its peak over the 10 year period 2002–2012 (Fig. 5). This time series shows that the artificial iron addition of 2012 stimulated the strongest chlorophyll anomalies evident over the past 10 years in this region. Its peak magnitude was over twice as high as that of the phytoplankton bloom fueled by the volcanic ash deposition of Kasatochi in 2008 and ~5 times that of 10-year climatological concentrations in the region, including any blooms associated with eddies that propagated through the region (Fig. 2).

To present the 2012 bloom magnitude in context of historical anomalies over the entire central GoA, using monthly mean images, at each pixel location we counted the number of months over the 2002–2012 period in which the surface chlorophyll concentration anomaly exceeded 1.5 mg m^{-3}. A 3 by 3 pixel median filter was first applied to each monthly image to reduce speckle noise associated with cloud edges and other atmospheric correction difficulties. Values reach ≥3 over the shelf and shelf break regions along the eastern edge and northwestern parts of our study area (Fig. 6). In the central GoA, however, only two events stimulated phytoplankton increases >1.5 mg m^{-3} over the past 10 years. A few pixels reach 2 in the area of the artificially-induced bloom. Examination of the image time series (not shown) indicated that these two events were the artificially-induced bloom and volcano-induced bloom. Apart from these, the central GoA is generally characterized by surface chlorophyll concentration anomalies less than 1.5 mg m^{-3}.

In addition to the temporal scale, the spatial scale of the volcano-induced bloom of 2008 was also significantly larger than the artificially-

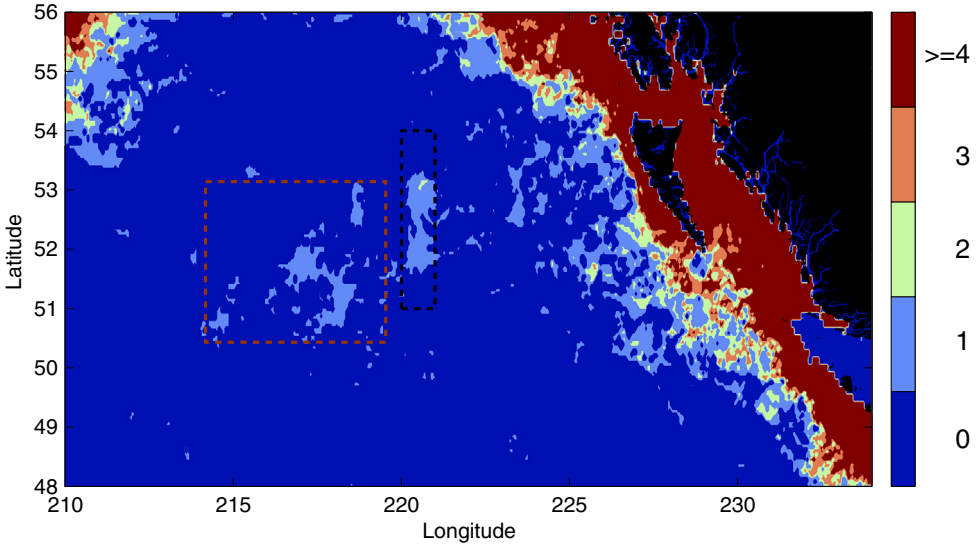

Fig. 6. Number of months when the chlorophyll concentration anomaly (calculated by subtracting climatological monthly mean) is higher than 1.5 mg m^{-3} during July 2002–November 2012 period. Black dashed rectangle marks the approximate position of artificially-induced bloom in 2012 and red dashed rectangle marks the approximate position of volcano-induced bloom in 2008.

induced bloom of 2012 (Fig. 7). The volcano-induced bloom covered almost the entire study region with chlorophyll concentration anomalies greater than 0.5 mg m^{-3}. The artificially induced bloom appeared to be confined to the local mesoscale eddy region but with stronger anomalies.

To further quantify and contrast the potential biological impact of these two blooms, we estimated the event-induced total upper ocean chlorophyll biomass for the late summer period of each year over the open basin (water depths > 3000 m) in the Haida region (see Fig. 2). We integrated total chlorophyll concentration over two months (sum of monthly data in August and September) and over the upper 40 m assuming a homogeneous vertical chlorophyll distribution over this depth range. This is a simplification, but does allow comparison. Measured mixed layer depths at station Papa (215°E, 50°N) have been shown to be ~40 m in these two months (Whitney & Freeland, 1999). The total integrated chlorophyll biomass was about 5.7×10^{10} g chlorophyll in the Haida region in 2008, and this number reduced to 3.3×10^{10} g chlorophyll in 2012. Assuming a constant phytoplankton chlorophyll-to-carbon ratio (0.02 g:g), and a iron-to-carbon ratio of 2.9 μmol:mol (Maldonado & Price, 1999), this would lead to total drawdown of 2.4×10^{11} mol of total CO_2 and 38.8 tons of dissolved iron in 2008, and 1.4×10^{11} mol of total CO_2 and 22.5 tons of dissolved iron in 2012, respectively. As the iron addition area was relatively small, the total carbon and iron uptake in 2012 was comparable to the 10-year climatological values (including 2008 and 2012), 1.3×10^{11} mol of total CO_2 and 21.3 tons of dissolved iron.

In the HNLC region where phytoplankton growth is under iron stress, iron addition can change phytoplankton physiology, increasing growth rates and phytoplankton chlorophyll-to-carbon ratios (Westberry et al., 2013). The satellite data suggest a much stronger increase of

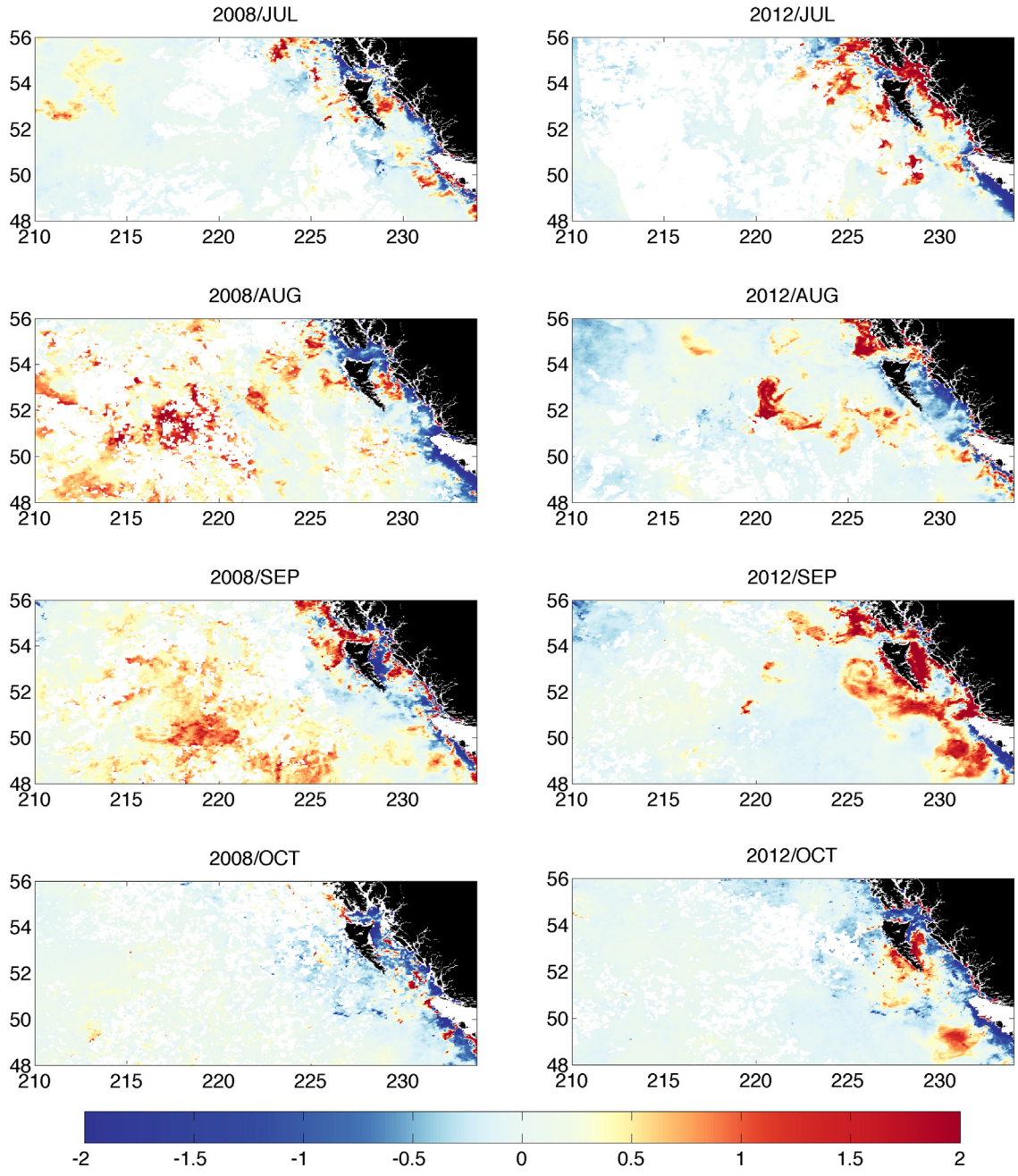

Fig. 7. Spatial distributions of monthly surface chlorophyll anomalies (mg m^{-3}) for July, August, September, and October in 2008, the year of volcanic iron input, and 2012, the year of the fertilization experiment.

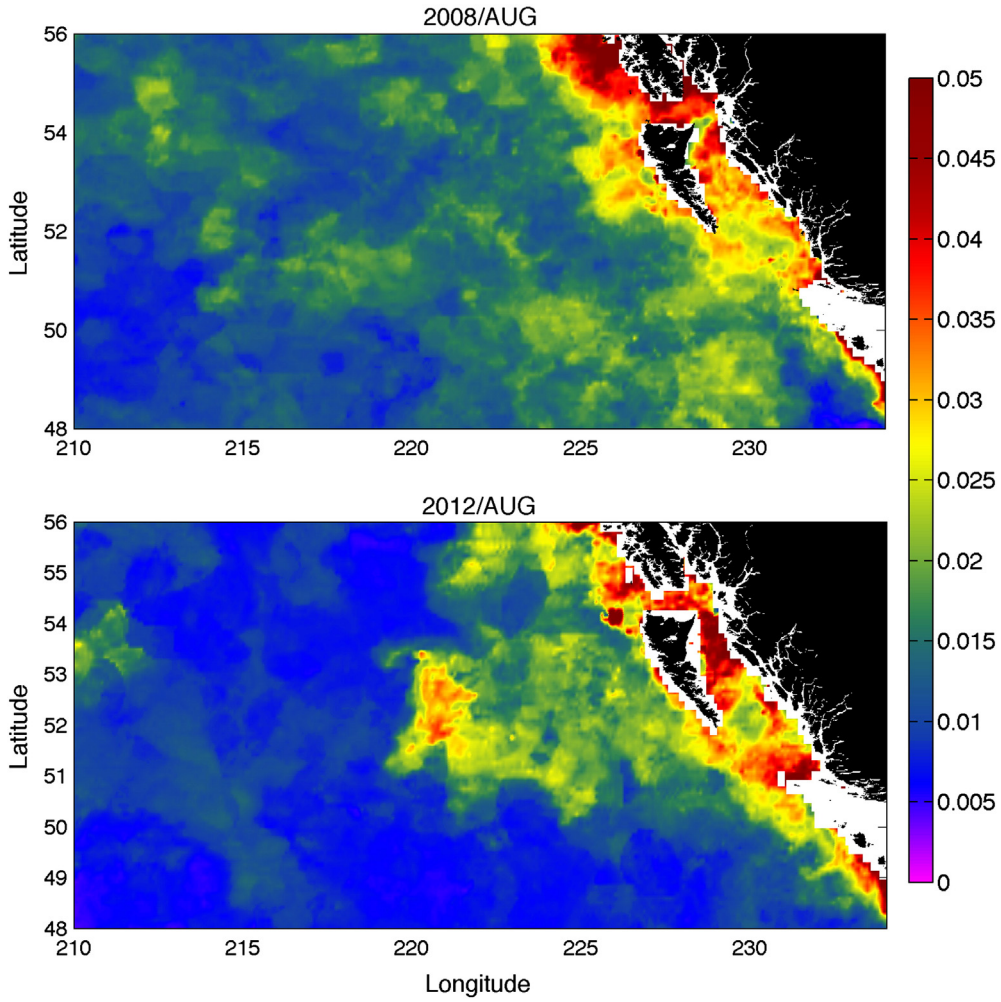

Fig. 8. Spatial patterns of phytoplankton chlorophyll-to-carbon ratios (g:g) in August 2008 and 2012.

phytoplankton Chl:C ratio in the 2012 artificial iron addition than in the 2008 Kasatochi volcanic addition (Fig. 8). Using these Chl:C ratios, total drawdown increased to 3.1×10^{11} mol of CO_2 and 49.7 tons of iron in 2008 (Table 2), and 1.8×10^{11} mol and 28.7 tons in 2012, respectively. The carbon and iron drawdown in 2008 in the Haida region was primarily caused by the broad impact of the Kasatochi volcanic iron addition (Fig. 7). This estimate is about half the Kasatochi volcano-induced total carbon drawdown in the GoA calculated by Hamme et al. (2010). However, our spatial integration area (9.3×10^5 km^2) is roughly half of theirs. In 2012, the artificially-induced bloom covered a relatively small area (Fig. 7). When considering this bloom area only, we estimated the drawdown of 1.84×10^{10} mol of CO_2 and 3.0 tons of iron induced by the artificially-induced bloom in 2012 (Table 2), which is about 16 times lower than the Kasatochi volcanic iron addition. This suggests that the 2012 artificially-induced bloom was relatively insignificant in terms of total iron drawdown (3.0 versus 28.7) for the Haida region as a whole. According to media reports, HSRC dumped over 100 tons of an iron-rich substance during the iron-addition experiment. These calculations suggest that only a small fraction of the dumped iron was biologically used and converted to organic matter. Weak eddy rotation likely enhanced the dispersal of iron into surrounding waters and/or contributed to sinking.

Whether or not increased iron availability and subsequent phytoplankton production from the eruption of Kasatochi volcano in 2008 were a significant contributor to a strong increase in recent sockeye salmon returns has been debated (McKinnell, 2013; Parsons & Whitney, 2012). In terms of total annual carbon drawdown, this natural event is comparable to the mesoscale Haida eddies (Table 2). The annual carbon drawdown by mesoscale Haida eddies shown in the table was calculated assuming a continuous vertical iron injection over the year (Xiu et al., 2011). While the 2012 dumping event resulted in strong localized chlorophyll anomalies, its total annual carbon drawdown is much lower than that of the Kasatochi volcano because of its small spatial coverage, and also smaller than that of annual mesoscale eddies because of its short duration. Given the eddy's weak rotation and the experiment timing in relation to seasonal patterns of higher trophic levels

Table 2
Estimated total drawdown of chlorophyll, carbon, and dissolved iron for different events in the Haida region. Both chlorophyll and carbon in 2008 and 2012 events are obtained from satellite measurements.

Events	Total chlorophyll (g Chl)	Total carbon (mol C)	Total iron (metric ton)
Kasatochi in 2008	5.7×10^{10}	3.1×10^{11}	49.7
Iron addition in 2012 (iron addition area only)	6.1×10^{9}	1.8×10^{10}	3.0
Eddies each year[a]		0.1×10^{12}–3.5×10^{12}	19.6–486.6
Seasonal drawdown[b]		1.3×10^{12}	

[a] Xiu et al. (2011).
[b] Wong et al. (2002).

(e.g., salmon age structure, locations, and age specific feeding preferences), the extent to which the iron-addition experiment might increase future salmon returns remains difficult to assess.

4. Conclusions

Due to the HNLC nature of the GoA, iron plays a critical role in modulating phytoplankton processes, ocean productivity, and carbon cycling. Publically available satellite data suggests that the privately funded iron fertilization experiment of August 2012 was conducted in an eddy with a characteristic life history and trajectory, but relatively weak circulation. It stimulated an anomalous phytoplankton bloom that was locally stronger than the bloom caused by natural iron input in September 2011. The experiment also created elevated turbidity for an extended period. At its location in the central GoA, this experiment induced the largest phytoplankton bloom observed over the past 10 years, even stronger than that caused by iron addition associated with the Kasatochi volcano in 2008. Due to its limited spatial and temporal scales, in terms of broad impacts, however, estimated total annual carbon drawdown by this experiment is an order of magnitude smaller than that of the Kasatochi volcano and annually recurring Haida eddies. By September 2012, the artificially created biological realm had started to disperse into surrounding waters. This, in addition to cloudy periods, created difficulties for the visible satellite data to continue to quantitatively monitor phytoplankton chlorophyll patterns associated with the event. In the future, the combination of observations (satellite and in-situ), numerical models, as well as new approaches would be required to quantify the full impact of iron addition on ocean productivity, biogeochemical cycles, and any response of the ecosystem, especially at higher trophic levels, and over extended periods.

Acknowledgments

Funding for this work was provided by the open fund of the State Key Laboratory of Tropical Oceanography (South China Sea Institute of Oceanology, Chinese Academy of Sciences) (LTO1107) (PX), the 100-Talent Program of Chinese Academy of Sciences (PX), the Strategic Priority Research Program of the Chinese Academy of Sciences, XDA10010304 (PX), NASA NNX10AU07G (ACT), NASA NNX09AU39G (FC), NSF OCE-0814413, OCE0815051 (ACT) and OCE-0961345 (FC) and the University of Maine. We thank the NASA ocean color team for access to the MODIS data and CNES/AVISO for access to the satellite altimeter products.

References

Behrenfeld, M. J., Westberry, T. K., Boss, E. S., O'Malley, R. T., Siegel, D. A., Wiggert, J.D., et al. (2009). Satellite-detected fluorescence reveals global physiology of ocean phytoplankton. *Biogeosciences*, *6*, 779–794.

Bishop, J. K. B., Davis, R. E., & Sherman, J. T. (2002). Robotic observations of dust storm enhancement of carbon biomass in the North Pacific. *Science*, *298*, 817–821.

Boyd, P. W., Jickells, T., Law, C. S., Blain, S., Boyle, E. A., Buesseler, K. O., et al. (2007). Mesoscale iron enrichment experiments 1993–2005: Synthesis and future directions. *Science*, *315*, 612–617.

Boyd, P. W., Law, C. S., Wong, C. S., Nojiri, Y., Tsuda, A., Levasseur, M., et al. (2004). The decline and fate of an iron-induced subarctic phytoplankton bloom. *Nature*, *428*, 549–553. http://dx.doi.org/10.1038/nature02437.

Boyd, P., Wong, C. S., Merrill, J., Whitney, F., Snow, J., Harrison, P. J., et al. (1998). Atmospheric iron supply and enhanced vertical carbon flux in the NE subarctic Pacific: Is there a connection? *Global Biogeochemical Cycles*, *12*, 429–441.

Chelton, D. B., Gaube, P., Schlax, M. G., Early, J. J., & Samelson, R. M. (2011). The influence of nonlinear mesoscale eddies on near-surface oceanic chlorophyll. *Science*, *334*, 328–332.

Coale, K. H., Johnson, K. S., Chavez, F. P., Buesseler, K. O., Barber, R. T., Brzezinski, M.A., et al. (2004). Southern ocean iron enrichment experiment: Carbon cycling in high- and low-Si waters. *Science*, *304*, 408–414.

Combes, V., Di Lorenzo, E., & Curchitser, E. (2009). Interannual and decadal variations in cross-shelf transport in the Gulf of Alaska. *Journal of Physical Oceanography*, *39*, 1050–1059.

Crawford, W. R. (2002). Physical characteristics of Haida Eddies. *Journal of Oceanography*, *58*, 703–713.

Crawford, W. R. (2005). Heat and fresh water transport by eddies into the Gulf of Alaska. *Deep-Sea Research II*, *52*, 893–908.

Crawford, W. R., Brickley, P. J., & Thomas, A.C. (2007). Mesoscale eddies dominate surface phytoplankton in northern Gulf of Alaska. *Progress in Oceanography*, *75*, 287–303.

de Baar, H. J. W., Boyd, P. W., Coale, K. H., Landry, M. R., Tsuda, A., Assmy, P., et al. (2005). Synthesis of iron fertilization experiments: From the Iron Age in the Age of Enlightenment. *Journal of Geophysical Research*, *110*, C09S16. http://dx.doi.org/10.1029/2004JC002601.

Duce, R. A., & Tindale, N. W. (1991). Atmospheric transport of iron and its deposition in the ocean. *Limnology and Oceanography*, *36*, 1715–1726.

Feldman, G. C., & McClain, C. R. (2009). Ocean Color Web, MODIS-Aqua Reprocessing 2009.1, NASA Goddard Space Flight Center. In N. Kuring, & S. W. Bailey (Eds.), (2013. http://oceancolor.gsfc.nasa.gov/.).

Hamme, R. C., Webley, P. W., Crawford, W. R., Whitney, F. A., DeGrandpre, M.D., Emerson, S. R., et al. (2010). Volcanic ash fuels anomalous plankton bloom in subarctic northeast Pacific. *Geophysical Research Letters*, *37*, L19604. http://dx.doi.org/10.1029/2010GL044629.

Henson, S. A., & Thomas, A.C. (2008). A census of oceanic anticyclonic eddies in the Gulf of Alaska. *Deep-Sea Research I*, *55*, 163–176.

Jickells, T. D., An, Z. S., Andersen, K. K., Baker, A.R., Bergametti, G., Brooks, N., et al. (2005). Global iron connections between desert dust, ocean biogeochemistry, and climate. *Science*, *308*, 67–71.

Johnson, W. K., Miller, L. A., Sutherland, N. E., & Wong, C. S. (2005). Iron transport by mesoscale Haida eddies in the Gulf of Alaska. *Deep-sea Research II*, *52*, 933–953.

Ladd, C. (2007). Interannual variability of the Gulf of Alaska eddy field. *Geophysical Research Letters*, *34*, L11605. http://dx.doi.org/10.1029/2007GL029478.

Lam, P. J., Bishop, J. K. B., Henning, C. C., Marcus, M.A., Waychunas, G. A., & Fung, I. Y. (2006). Wintertime phytoplankton bloom in the subarctic Pacific supported by continental margin iron. *Global Biogeochemical Cycles*, *20*, GB1006. http://dx.doi.org/10.1029/2005GB002557.

Lukacs, M. (2012). World's biggest geoengineering experiment 'violates' UN rules. The Guardian, October 15, 2012. http://www.theguardian.com/environment/2012/oct/15/pacific-iron-fertilisation-geoengineering.

Maldonado, M. T., & Price, N. M. (1999). Utilization of iron bound to strong organic ligands by plankton communities in the subarctic Pacific Ocean. *Deep-Sea Research II*, *46*, 2447–2473. http://dx.doi.org/10.1016/S0967-0645(99)00071-5.

Martin, J. H. (1990). Glacial-interglacial CO_2 change: The iron hypothesis. *Paleoceanography*, *5*, 1–13.

McKinnell, S. (2013). Challenges for the Kasatochi volcano hypothesis as the cause of a large return of sockeye salmon (Oncorhynchus nerka) to the Fraser River in 2010. *Fisheries Oceanography*, *22*(4), 337–344.

Morel, A., & Gentili, B. (2009). A simple band ratio technique to quantify the colored dissolved and detrital organic material from ocean color remotely sensed data. *Remote Sensing of Environment*, *113*, 998–1011.

Nishioka, J., Takeda, S., Wong, C. S., & Johnson, W. K. (2001). Size-fractionated iron concentrations in the northeast Pacific Ocean: Distribution of soluble and small colloidal iron. *Marine Chemistry*, *74*, 157–179. http://dx.doi.org/10.1016/S0304-4203(01)00013-5.

Parsons, T. R., & Whitney, F. A. (2012). Did volcanic ash from Mt. Kasatoshi in 2008 contribute to a phenomenal increase in Fraser River sockeye salmon (Oncorhynchus nerka) in 2010? *Fisheries Oceanography*, *21*, 374–377.

Service, R. F. (2012). Legal? Perhaps. But controversial fertilization experiment may produce little science. ScienceInsider, October 23, 2012. http://news.sciencemag.org/2012/10/legal-perhaps.-controversial-fertilization-experiment-may-produce-little-science?ref=hp.

Stabeno, P. J., Bond, N. A., Hermann, A. J., Kachel, N.B., Mordy, C. W., & Overland, J. E. (2004). Meteorology and oceanography of the Northern Gulf of Alaska. *Continental Shelf Research*, *24*, 859–897.

Strutton, P. (2012). Mixing iron into the north Pacific stirs geo-engineering controversy. The Conversation, November 8, 2012. http://theconversation.edu.au/mixing-iron-into-the-north-pacific-stirs-geo-engineering-controversy-10490.

Thomas, A.C., & Weatherbee, R. A. (2006). Satellite-measured temporal variability of the Columbia River plume. *Remote Sensing of Environment*, *100*, 167–178.

Tollefson, J. (2012, 23 October). Ocean-fertilization project off Canada sparks furore. *Nature*, *490*, 458–459. http://dx.doi.org/10.1038/490458a (http://www.nature.com/news/ocean-fertilization-project-off-canada-sparks-furore-1.11631).

Westberry, T. K., Behrenfeld, M. J., Milligan, A. J., & Doney, S.C. (2013). Retrospective satellite ocean color analysis of purposeful and natural ocean iron fertilization. *Deep-Sea Research I*, *73*, 1–16.

Westberry, T. K., Behrenfeld, M. J., Siegel, D. A., & Boss, E. (2008). Carbon-based primary production modeling with vertically resolved photoacclimation. *Global Biogeochemical Cycles*, *22*, GB2024. http://dx.doi.org/10.1029/2007GB003078.

Whitney, F. A., & Freeland, H. J. (1999). Variability in upper-ocean water properties in the NE Pacific Ocean. *Deep-Sea Research II*, *46*, 2351–2370.

Wong, C. S., Waser, N. A.D., Nojiri, Y., Whitney, F. R., Page, J. S., & Zeng, J. (2002). Seasonal cycles of nutrients and dissolved inorganic carbon at high and mid latitudes in the North Pacific Ocean during the Skaugran cruises: Determination of new production and nutrient uptake ratios. *Deep-Sea Research II*, *49*, 5317–5338. http://dx.doi.org/10.1016/S0967-0645(02)00193-5.

Xiu, P., Chai, F., Xue, H., Shi, L., & Chao, Y. (2012). Modeling the mesoscale eddy field in the Gulf of Alaska. *Deep-Sea Research I*, *63*, 102–117.

Xiu, P., Palacz, A. P., Chai, F., Roy, E. G., & Wells, M. L. (2011). Iron flux induced by Haida eddies in the Gulf of Alaska. *Geophysical Research Letters*, *38*, L13607. http://dx.doi.org/10.1029/2011GL047946.